ADELAIDE UNIVERSITY

Geology and Geophysics

The Poodla Granite in the Olary Domain, South Australia: Intrusive Relationships, Alteration and implications for Cu-Au mineralisation

Justin L. Payne

Supervisors: Andreas Schmidt-Mumm

John Foden

November 2003

This paper is submitted as partial fulfilment for the Honours degree of Bachelor of Science (Geology)

CONTENTS

LIST OF FIGURES

LIST OF TABLES

ABSTRACT

The Palaeoproterozoic Poodla Granite within the Olary Domain, Curnamona Province, South Australia, has been suggested as a direct contributor to Cu-Au mineralisation within the region on the basis of age correlations.

Alteration present within the Poodla Granite consists of four styles that have been interpreted as two events. The first event includes pervasive potassic alteration followed by pervasive Na-Ca alteration. Sm/Nd isotope analysis indicates fluids for this event were sourced from the Willyama Supergroup sediments. The second event consists of fracture-controlled sodic and Ca-Na-Si alteration with associated actinolite/clinopyroxene brecciation. Utilisation of magmatic major element trends obtained from a natural analogue (Mt Angelay Complex, Cloncurry District) has allowed greater accuracy in chemical characterisation of alteration. Fluid inclusion analysis has identified two distinct fluids involved in the later fracture-controlled sodic and Ca-Na-Si alteration event. Namely, a low salinity (18-26wt% NaCl equivalent) and a high salinity (35-45wt% NaCl equivalent) fluid. A later fluid mobilisation event related to the Palaeozoic Delamerian Orogeny is indicated by re-equilibration of the Rb/Sr isotopic system.

New age constraints from other granites in the I-type suite, to which Poodla Granite belongs, suggest the Poodla Granite did not have direct hydrothermal input into regional Cu-Au mineralisation. Analysis of alteration chemistry suggests that Cu and Au mobilisation occurred during the first alteration event. These results offer evidence for

previously untested Cu-Au mineralising models within the region and may encourage exploration for Cu-Au resources.

Key Words : Curnamona Province, I-type granite, Alteration, Cu-Au mineralisation

1. INTRODUCTION

The Curnamona Province, situated in north-eastern South Australia and eastern New South Wales (Figure 1), hosts the giant Broken Hill Pb-Zn-Ag deposit and a number of small Cu-Au occurrences, including the White Dam, Luxemburg, Kalkaroo, Green and Gold and Portia mineralisations (Robertson et al., 1998). It is thought however that the Olary Domain, in particular, is under-explored with respect to other equivalent Proterozoic terrains. Correlations with the Cu-Au rich (eg. Ernest Henry and Eloise) Cloncurry/Mt Isa region, based on sediment provenance, geochronological and lithological similarities (Page et al., 2000; Barovich et al., 2002), support the suggestion that undiscovered Cu-Au mineralisation exists in the Olary Domain.

Cu-Au mineralisation has been extensively linked to magmatic activity, such as at Olympic Dam (Johnson and McCulloch, 1995; Ferris et al., 2002) and in the Cloncurry region (Wyborn, 1998; Pollard et al., 1998). Six Palaeo- and Mesoproterozoic igneous suites are currently recognized in the Olary Domain. A suite of I-type granitoids has been suggested as instigating Cu-Au mineralisation systems by providing fluids and/or thermal energy. This was founded upon correlations between crystallisation ages of the

granites and known Cu-Au mineralisation ages (~1632-1612 Ma, Kalkaroo, Skirrow et al., 1999). The I-type suite includes the Poodla, Antro and Tonga granitoids and a small occurrence west of Alconie Hill (informally referred to here as South Willow). Intrusive ages for the granites include 1641 ± 11 Ma for Antro (Ashley et al., 1997) and 1629 ± 12 Ma for Poodla (Cook et al., 1994). Based on recent SHRIMP zircon U-Pb investigations, Page et al. (2003) suggest that at least part of Poodla has a Basso Suite crystallisation age (ca. 1710 Ma) and suggest a Lady Louise age (ca. 1685 Ma) for Antro. Meta-sediment enclaves within the granite have previously been reported to contain a pre-intrusion foliation, suggesting a younger, post-deformation age (Ashley et al., 1998). Hence ambiguity still surrounds the crystallisation and emplacement ages of the suite, which has important implications for mineralisation scenarios.

Field and laboratory studies have been conducted to determine relative ages of the Poodla Granite emplacement, intrusive suite affinities and alteration. As the Poodla Granite has undergone several alteration events (Hill, 1995), it provides an excellent opportunity to study the characteristics of these events and their relationships to alteration and mineralisation previously described in the region (eg. Ashley et al., 1998; Kent et al., 2000; Skirrow et al., 2003). The results from this study are combined with existing knowledge of the region and known Cu-Au provinces to provide a better understanding of the significance of these events in the Olary Domain.

2. REGIONAL GEOLOGY

The Olary Domain (Figure 1) of the Curnamona Province consists of a sequence of Palaeoproterozoic meta-sedimentary and meta-volcanic units, which have been intruded by Palaeo- and Mesoproterozoic igneous suites. Previous studies describing the geology of the Olary Domain are summarised by Clarke et al. (1986, 1987), Flint and Parker (1993), Robertson et al. (1998), Conor (2000) and Raetz et al. (2002). The stratigraphy and lithological relationships of the Olary Domain are summarised in Figure 2.

The Proterozoic stratigraphic succession of the Olary Domain, the Willyama Supergroup, is divided into the basal Curnamona and upper Strathearn Group. The Curnamona Group is further subdivided into two subgroups. The lower of the two, the Wiperaminga Subgroup, consists of quartzofeldspathic schists, gneisses and migmatites. The upper, Ethiudna Subgroup, is more lithologically diverse, characterised by carbonate/calcsilicate, pyritiferous pelites and fine albitic psammitic lithologies. The Strathearn Group is separated from the Curnamona Group by the Bimba Formation and the overlying tuffaceous 'Plumbago Formation' (1692±3 Ma, Page et al., 2003). The 'Plumbago Formation' represents a short interval of deposition during what is otherwise a hiatus of sedimentation (Conor, 2003). At different localities within the domain the Saltbush and Mount Howden Subgroups variably overlie the 'Plumbago Formation'. These subgroups are dominantly pelite to psammopelite with minor interbedded thin psammite layers.

Coeval with deposition of the Curnamona Group is the widespread Basso Suite of subvolcanic intrusives, volcanics and epiclastics (~1715-1707 Ma). This suite has been classified as A-type (Benton, 1994; Ashley et al., 1996), generally has elevated SiO_2 (>73 wt%) and low Al_2O_3, TiO_2, CaO, P_2O_5, Sr and Eu. Differentiated mafic sills within the Ethiudna Subgroup constitute the intrusive Lady Louise Suite (ca. 1685 Ma, Conor, 2003). This suite is dominated by amphibolite (amphibole, plagioclase and epidote) with the occurrence of granitic end-member intrusives consisting largely of quartz and plagioclase with biotite, hornblende, magnetite, rutile and titanite.

Granitoids interpreted as I-types are relatively limited in their distribution within the domain. Bodies at Antro, Tonga Hill, west of Alconie Hill (South Willow) and Poodla have all experienced variable alkali (Na, K) and 'calc-silicate' alteration (Conor, 2003). Antro is classified as a tonalite and consists of plagioclase (~55%), quartz (~25%), clinopyroxene (~15%) and K-feldspar (<5%), with minor titanite and apatite (Benton, 1994). The South Willow and Poodla syenogranites (Freeman, 1995; Hill, 1995) are mineralogically and chemically similar. South Willow contains K-feldspar (45%), quartz (20%), biotite (15%), magnetite (~7%), titanite (5%), epidote (5%) and zircon (<1%) (Freeman, 1995). The Antro and Poodla granitoids have yielded SHRIMP zircon U-Pb ages of 1641±11 Ma (Ashley et al., 1997) and 1629±12 Ma (Cook et al., 1994) respectively. More recent SHRIMP zircon U-Pb investigations by Page et al. (2003) have indicated a Basso Suite crystallisation age (ca. 1710 Ma) for at least part of Poodla, and a Lady Louise age (ca. 1685 Ma) for Antro.

Regional S-type granites of the Bimbowrie Supersuite, intruded shortly after the Olarian Orogeny (~1580 Ma, Cook et al. 1994) (Conor, 2000). These range in composition from 2-mica monzogranites to biotite-hornblende bearing quartz monzodiorites. Contact relations encompass sharp intrusive to gradational zones and migmatites. Unlike the older intrusives in the region, the Bimbowrie Supersuite has seen very limited alteration and is un- to superficially foliated (Conor, 2003).

The current understanding of the structural history of the Olary Domain identifies two major orogenic events, the Proterozoic Olarian and Palaeozoic Delamerian orogenies, comprising six deformations in total. The first orogenic event may also have been preceded by early low angle shearing producing layer parallel mylonite zones (Noble et al., 2003).

The first of the orogenic events, the Olarian (OD1-OD4, Table 1), occurred from approximately 1600 to 1580 Ma, involving extensive crustal shortening and related S-type granite magmatism. The later Palaeozoic Delamerian orogeny (DD1-DD2, ~500Ma) is the predominant orogenic event in the surrounding/overlying Adelaidean Neoproterozoic sediments. This orogenic event resulted in tightening of the Olarian structures and overprinting of metamorphic mineral assemblages, particularly in the southern inliers of the Olary Domain. Its effects decrease towards the north.

3. RESULTS

Structural mapping has been conducted to determine the tectonic evolution of the study area. To further characterise the primary composition and alteration chemistry of the rock types in the area, a representative suite of samples has been analysed by X-ray fluorescence (XRF) for whole rock major and trace elements. Alteration mineral assemblages have been analysed by electron microprobe to determine the chemical evolution of alteration fluids. Sm/Nd and Sr isotopic analysis was undertaken to determine the sources of magmas and alteration fluids. Microthermometric fluid inclusion analysis was carried out to establish the chemical composition and physical conditions of alteration fluids.

3.1 Structural setting and relative age constraints of the Poodla Granite area

The Poodla Granite outcrops along the eastern edge of southern Telechie Valley (Figure 3) and is interpreted to be more extensive under cover from aero-magnetics and radiometrics. The granite outcrops in the Wiperaminga Subgroup and has experienced deformation and multiple brecciation and alteration events.

Extensive brecciation along the northern, north-western and southern granite/meta-sediment contact has obscured contact relations; elsewhere the contact is not exposed, being prone to weathering, or under cover.

Mapping of the Poodla Granite and surrounding metasediments (Figure 3) established a scheme for the structural evolution of the area, particularly the relationship between the granite body and its host rock. Evidence of 5 deformation events is found in the area, a summary of which can be found in Table 2.

The granite body has acted very much as a rigid object due to its much higher competence than the surrounding metasediments. This is evidenced by the lack of deformation within the granite and the development of a 'pressure-shadow' directly to the north of the granite. In this 'shadow' (Figure 4b) deformation of the metasediments is highly variable with much less correlation of structural orientations evident.

The lithologies surrounding the Poodla Granite are strongly affected by the Olarian Orogeny. Layer-parallel foliation (S1) in the meta-sediments is extensively developed and has been traditionally associated with the OD1 event. This association is confirmed in this study, as the S1 foliation is deformed by all later events. Rare examples of OF2 folds or fold hinges are seen refolded by the later OD3 shortening event. These folds have been tightened in the hinges of mesoscopic OF3 folds, but appear to have been tight initially.

Regional scale and mesoscopic folding (Figure 4a) is attributed to the dominant OD3 event, producing the prevailing structural orientations seen within the study area (Figure 4b). This event also produced axial planar cleavage and crenulation of earlier layer-parallel foliation. Folds are characterised as moderate to tight, steeply plunging with a NE-SW trend. Variable plunge is found in mesoscopic folds due to differing

competency of psammite and pelite layers. The granite is positioned in the core of a regional-scale OF3 synform. Shearing along the northern margins of the granite is related to a south-east up mylonite zone running along the eastern edge of the Telechie Valley. This mylonite occurs in the Ethiudna Subgroup metasediments and runs along or close to the Wiperaminga/Ethiudna Subgroup contacts. The plane of shear (042/70 NW) and mineral elongation lineations are plotted in Figure 4c. This shearing is linked to the OD4 event. Minor mesoscopic E-W trending folds (Figure 4a) are also attributed to OD4. Later folding is attributed to the Delamarian Orogeny, and is seen to plunge moderately to steeply to the SSE (Figure 4a).

3.1.1 PETROGRAPHIC ANALYSIS OF META-SEDIMENTARY ENCLAVES

Numerous angular to sub-angular, meta-sedimentary enclaves are found within the granite body. These had previously been reported by Ashley et al. (1998) to be foliated prior to granite intrusion, raising questions concerning the validity of the absolute age data. Oriented thin sections were made of enclaves to enable comparison to metamorphic fabrics seen in the surrounding meta-sediments. Enclaves were sampled to give the greatest rotation of orientation of any possible pre-intrusion fabrics relative to the latter OD3 and OD4 fabrics. Careful selection and examination of 2 oriented enclave sections and 2 oriented meta-sediment sections was undertaken. One of the enclaves, the most pelitic, contains no foliation, pre-intrusion or otherwise. Mineralogy consists of fine-grained quartz, biotite and plagioclase. The second enclave exhibits one foliation. This enclave shows growth of muscovite porphyroblasts prior to the development of foliation. Muscovite blasts are randomly orientated and some possess stress shadows of

later biotite. It is this biotite growth that defines the foliation present in the enclave. Orientation of the foliation is 54/62NW, which falls within expected deviation of fabrics related to OD3 and OD4. This observation is supported by the metamorphic assemblage, which cannot be considered typical of the early layer-parallel foliation within the Olary Domain.

3.2 Breccia

Considerable variation of matrix and clast composition and clast/matrix ratios occurs in the breccia found in the study area. Two genetic groups are distinguished based upon mineralogical composition of the matrix, biotite-matrix and actinolite/clinopyroxene-matrix breccias. Genesis of breccias elsewhere in the Olary Domain is described by Clark and James (2003).

The dominant breccia type within the granite is a matrix supported, fine-grained biotite, magnetite, albite and quartz breccia, termed biotite-matrix breccia. This breccia outcrops extensively along the granite/meta-sediment contact, within the granite and, to a lesser extent, in the meta-sediments directly to the north-east of the granite (Figure 3). Clasts consist of albite and quartz-albite with minor biotite and are presumably albitised meta-sediments. Clasts are dominantly inter-formational and range in size from 2mm to 15mm and are typically sub-rounded. Breccia bodies within the granite also contain minor granite clasts <1%. Similar breccias reported elsewhere in the Olary Domain are structurally controlled in OF3 fold hinges (Clark and James, 2003). Heterogenous foliation of the breccia is linked to OD4 shearing. Biotite-matrix breccia is not included

in Table 2 as its timing is unclear. Field evidence, such as foliated biotite-matrix breccia in contact with unfoliated actinolite/clinopyroxene breccia, indicates it occurred prior to OD4 and OD3 or early syn-OD3. The presence of albitic clasts indicates it is likely to have occurred after the pervasive Na-Ca alteration seen in the meta-sediments. This however, cannot be considered conclusive, as the origin of the inter-formational clasts is unknown.

The second breccia type, an actinolite/clinopyroxene matrix breccia, is the more widespread of the two breccia types, occurring in the area directly north of the granite (Figure 3) and along the Telechie Valley as prominent outcrops of brecciated Ethiudna Subgroup. This breccia has significant variation of matrix composition and grain size. Grain size varies from fine (<3mm) to coarse (3-10mm). Clasts are predominantly in-situ and are composed chiefly of albite and calc-silicate minerals. The breccia is unfoliated and also contains rafts of mylonite (from an unknown source). Sodic alteration surrounds larger breccia bodies, also associated are quartz-actinolite veins with actinolite crystal growth up to 10cm in length. Breccias at Cathedral Rock, of similar matrix composition, are explosive in-situ breccias, structurally controlled by OD3 structures (Clark & James, 2003).

3.3 Petrographical, whole rock and mineral analysis of Poodla Granite

Eighteen un-weathered granite samples were analysed for whole rock major and trace element composition. Approximately 2kg of each was crushed to account for as much heterogeneity within the rock as practicable. Samples were milled in a WC mill and

analysed using a Phillips PW 1480 XRF. The data are presented in Table 3. Au analysis (fire assay, AAS) of selected samples was carried out by Amdel. Mineral compositions were analysed using the Cameca SX51 electron microprobe at Adelaide Microscopy at the University of Adelaide.

The granite is a medium-grained syenogranite with moderate internal variation of chemistry and mineralogy. Primary mineralogy typically consists of K-feldspar (~45%), quartz (20%), biotite (~15%), plagioclase (~10%), magnetite (~5%), titanite (~5%) and zircon (<1%). SiO_2 within the granite samples varies from 63 to 69 wt%, making it one of the most mafic (silica poor) granitoids in the region. Approximately 2 wt% (63-65 wt%) variation of silica is attributed to magmatic fractionation and crystallisation, the rest to variable levels of alteration.

Bierlein (1995) suggested trace element patterns remain constant during all but the highest degrees of alteration and metamorphism in the Curnamona Province. Data collected during this study indicates mobility of trace elements is limited but does occur during alteration. During the highest levels of depletion and recrystallisation, significant changes occur. Primitive mantle normalised incompatible element plots ("spidergrams", Figure 6a and 6b) allow comparison with other Olary intrusives and are also used to highlight the mobility of elements. Figure 6a depicts typical trace element compositions of Poodla, South Willow, Antro and Basso Suite intrusives. The Cloncurry Region, Mt Angelay Complex is also included in Figure 6a for later reference in Section 3.4.1. Poodla and South Willow are seen to share very similar incompatible element characteristics, indicating they are products of the same magma generation event. Antro

shows a relative Rb, Ba and K depletion and a minor Th depletion compared to Poodla and South Willow. This is in agreement with Freeman (1995), who suggested these characteristics were a result of post-magmatic alteration. Other minor differences between the two 'spidergram' plots are likely due to general fractionation and variation found within suites.

In Nb/Y tectonic discrimination diagrams Poodla plots as a 'within-plate granite' (Figure 7a). Previous studies have suggested the granite to have I-type affinities (Benton, 1994). This was based upon the presence of primary titanite, low Aluminium Saturation Index (ASI) and Ga/Al based S-, I- and A-type discrimination diagrams (Benton, 1994). Sampling and analysis conducted during this study indicates ASI values to be above 1.1 (per-aluminous, Figure 7b), characteristic of S- or A-type, and, upon re-plotting, modern Ga/Al based S-, I- and A-type discrimination diagrams prove unsuitable for classification. On the Ga/Al based diagrams of Whalen et al. (1987), Figure 7c, the majority of Olary granitoids plot as A- or transitional A/S-type rocks. As Poodla is extensively altered and classification methods are based on unaltered modern and late Phanerozoic magmatic systems their applicability will always be limited. Although not proving suitable for traditional classification of intrusives, some delineation between different suites is shown on these diagrams.

3.4 Alteration

The Poodla Granite has experienced several episodes of alteration of differing styles, each of which can be identified at macro- and microscopic scale. These are potassic, pervasive Na-Ca, and fracture-controlled sodic and Ca-Na-Si stages. Field relationships and mineral intergrowth and alteration are used to establish the sequence of alteration events in the granite.

Potassic alteration can be identified in the granite by aggregate growths of biotite typically 2-10mm in diameter, interspersed with and overgrowing primary biotite, usually less than 2mm in size. On a microscopic scale biotite veining is also evident (Figure 5a). The biotite shows typical pale to medium brown colouring under plane polarised light, indicative of its generation. The extent of potassic alteration is variable within the granite, but rarely extends into the host metasediments.

Pervasive Na-Ca alteration is found within the granite and, selectively, in psammite layers of the Wiperaminga metasediments within the study area. This Na-Ca alteration is expressed in the granite as general bleaching and variable, sometimes near-complete albitisation. Microscopically it is seen to alter K-feldspar to albite (Figure 5b, Table 4), produce minor epidote and alter biotite to a slightly K and Ti depleted composition (Table 4), pale green under plane-polarised light.

The second sodic alteration style is much more localised and controlled primarily by OD3 structures, such as axial planar cleavage, foliation and spaced cleavages. Within

the granite fracture-controlled alteration is seen to overprint the early potassic and Na-Ca alteration and commonly occurs as bands of progressively bleached/albitised rock around quartz and albite filled fractures (Figure 5c).

Ca-Na-Si alteration has been referred to as calc-silicate alteration by various authors (eg. Kent et al., 2000; Conor, 2003). It is referred to here as Ca-Na-Si alteration, in relation to its effects within the granite. Ca-Na-Si alteration is relatively limited within the granite, localised along fractures and in the vicinity of larger (up to 1m thick) quartz-actinolite veins. This alteration produced actinolite, tremolite, epidote, albite and bladed ilmenite (since altered to leucoxene, 97.4% TiO_2, 1.2% $Fe_2O_{3(T)}$) within microscopic veins of Mg-rich biotite ($Mg:Fe^{2+}$= 2.13). Field relationships, visibly related progression of alteration and remobilisation, in meta-sediments (Figure 5d) suggest the Ca-Na-Si alteration is a result of evolving fluids related to the fracture-controlled sodic event rather than a separate event.

3.4.1 CHEMICAL ANALYSIS OF ALTERATION

Investigations into the chemical effects of alteration must deal with the inherent problem of obtaining the original composition of the altered rock. Even once an acceptable unaltered composition is decided upon, mass balance constraints also need to be considered (Gresen, 1967), in order to quantify with any degree of certainty the movement of elements and species. The isocon diagram (Grant, 1986) is a graphical method for resolving Gresen's (1967) composition/volume relationships.

The compositional variation inherent to igneous rocks, even on the decimetre scale, means that determination of an unaltered rock composition has to make some allowance for the primary magmatic variability of the granite. However, the primary magmatic composition and fractionation trends of the granite can be estimated (modelled), and this 'primary' trend of element concentration used as a basis for determination of element mobility, a somewhat innovative combination of techniques. Major element concentrations, over a limited silica range, can be fitted to a linear model and trace elements to a Rayleigh model of fractionation.

As no completely unaltered samples were found in the Poodla granite, a natural analogue was considered to determine suitable fractionation trends of major and trace elements. The analogue used was the Proterozoic K-rich granitoids from the Mt Angelay Igneous Complex, Cloncurry District, Queensland, Australia (Mark, 1999). This complex varies in composition from metaluminous monzodiorite to subaluminous syenogranite and the suite contains magmas from two different sources. The felsic suite was chosen as a Poodla analogue as it shows similar composition and shares some trace element characteristics (Figure 6a). A linear line of best-fit was used to model the major element fractionation variations of the analogue, using silica as the abscissa. Silica concentrations in Poodla and the analogue were assumed to represent equivalent stages in magma evolution and fractional crystallisation. The modelled Rayleigh trace element fractionation trends were determined using appropriate distribution co-efficients (D). Trace element concentrations were found to have minimal variation in Poodla when compared to models produced by the analogue, and hence modelling their distribution would be inaccurate. The application of the major element fractionation values to

Poodla was done so as to pass the modelled magmatic evolution trend through the samples considered least altered for each element (PD1f and/or PD47, Figure 8a-h). This involved adjusting the vertical shift (y-axis intercept for linear models) of the model against an abscissa of silica. The validity of this method is demonstrated by the number of points falling along the induced fractionation line for elements that are generally considered immobile, particularly Al_2O_3. In cases such as K, it was felt justifiable to shift the line to a level considered more appropriate to pre-potassic alteration levels.

Model-magmatic compositions for each sample were thus obtained. Production of a model-magmatic composition for each sample allows investigation of the mass movement using isocon diagrams. In the particular cases where SiO_2 is thought to show a change in wt%, either through mobility or mass balance, a different silica value was assigned for development of the pseudo-magmatic composition. This is done to enable a more accurate initial composition to be constructed. Isocon diagrams for each sample (Figure 9) were plotted using TiO_2, Al_2O_3 and, where appropriate, SiO_2 as immobile elements (Grant, 1986). The slope of each isocon was multiplied with the calculated initial concentration of each element for its respective sample. This allows a much more accurate element addition/subtraction value to be obtained (Figure 10). Immobile trace elements were not considered in construction of isocons as they generally exhibit excessive variation in unaltered granite and inhibit accurate mass balance calculations. Despite this, isocon mass/gain values were still applied to trace element concentrations, as the mass balance effect is still present in the trace element concentrations.

Comparison of these concentrations was made to an average of samples PD1f and PD47 as unaltered trace element compositions.

Pervasive Na-Ca alteration in the granite is characterised by a distinct (~2 wt%) increase in Na, increase in Ca (~1.5 wt%), decrease in Mg (~0.5 wt%), decrease in Fe (~0.5 wt%), and a decrease in K (~1.4 wt%).

Ca-Na-Si alteration displays a somewhat contradictive range of chemical results. Based on the assumption that each sample has undergone previous pervasive Na-Ca alteration, an average Na increase of ~3.3 wt% is seen. K displays a decrease (~5.3 wt%) while Mg loss is negligible. The mass variations of Ca and Fe appear contradictory. PD20 shows a minor increase of Ca with respect to pervasive Na-Ca alteration samples, but no loss of Fe. PD41a and PD41b show what appears to be a decrease of Ca with respect to pervasive Na-Ca alteration samples and a significant Fe loss of 4.5 and 2.5 wt% respectively.

3.5 Fluid Inclusion Studies

Primary fluid inclusions associated with alteration events and secondary inclusions in oriented planes were analysed. Discrimination between primary, secondary and pseudo-secondary inclusions was based upon criteria from Van den Kerkhof and Hein (2001) and Roedder (1984). Primary inclusions were considered to be representative of the host-mineral forming fluid and also associated alteration, including alteration mineral assemblages in equilibrium with the inclusion-hosting quartz. Thermometric analysis

was conducted using a Linkam THMSG 600 heating and cooling stage. Measurements were taken via cycling to attain accurate T_m and T_h measurements repeatable at a ≤1˚C error value. Eutectic temperatures were recorded via repeated measurements at rates of 5˚C/minute, in some cases eutectics were recorded lower than a certain temperature, as actual first melting is indeterminable.

Inclusions from fracture-controlled sodic alteration and Ca-Na-Si alteration share similar fluid compositions: low salinity primary and secondary inclusions (Figure 11a) and high salinity 3-phase secondary inclusions (Figure 11b). Analysis of orientation of secondary inclusion planes for each fluid composition (Figure 4d) indicates coeval formation due to undifferentiable palaeo-stress regimes. The low salinity fluids (T_m -18.2 to -25.2°C, ~18-26wt% NaCl equiv., Table 6) indicate repeated injection of fluids, as they are present as both primary and secondary inclusions. This fluid shows eutectic temperatures of -37 ± 1˚C, suggesting influence of bivalent cations (eg. Ca^{2+}) in a predominantly monovalent (eg. Na^{+}) cation solution (Roedder, 1984). High salinity fluids (T_m -34.2 to -43.8°C, 35-45 wt% NaCl equiv.) tend to form larger secondary inclusions than their low salinity equivalents. Eutectic temperatures indicate a composition dominated by bivalent cations (eg. Ca^{2+}) with minor monovalent cations (eg. Na^{+}) (Roedder, 1984). Vapour homogenisation temperatures for inclusions found in quartz related to fracture-sodic alteration range from ~150-185°C for low-salinity inclusions and ~160-190°C for high-salinity inclusions. Solid phase dissolution in the high-salinity inclusions ranges from 240-285°C. Vapour homogenisation temperatures for Ca-Na-Si alteration range from 170-209°C for low salinity inclusions and 217-246°C for high salinity inclusions. Unlike the fracture-sodic alteration, solid dissolution

in the 3-phase inclusions occurs at lower temperatures than vapour homogenisation (~150-160°C).

3.6 Sm/Nd and Sr Isotopes

Sm/Nd and Sr isotopes of whole rock granite samples, considered representative of the unaltered granite as well as the different stages of alteration, were analysed to provide insight into possible magma and alteration fluid sources (Table 7). Samples analysed were PD1F (least altered sample), PD13 (pervasive Na-Ca alteration), PD15 (albitised–~90% albite) and PD41a (Ca-Na-Si altered).

The method used was that described by Elburg et al. (2003). Rock powders were dissolved through high-pressure dissolution bombs in HF and HNO_3. Sr was separated and concentrated in two passes through polyprep columns and Nd and Sm were separated on rare-earth element fractionation HDEHP columns. Sr and Nd isotopes were measured at the University of Adelaide on a Finnigan MAT 262 Thermal Ionisation Mass Spectrometer (TIMS) in static mode. Sm isotopes were measured on a Finnigan MAT 261. Sm/Nd samples were spiked with mixed ^{149}Sm-^{150}Nd spike and Rb/Sr with ^{84}Sr and ^{85}Rb spike. Blanks and an in-house standard (TasBas) monitored reproducibility and measured ratios indicated this to be better than 1% and 0.8% for Rb/Sr and Sm/Nd, respectively.

A Sr isochron (“error chron”) has been constructed (Figure 12). This isochron indicates an age of 540 ± 85 Ma as the homogenisation of the Rb-Sr isotope system. As indicated

in Figure 12, the mean squares weighted deviation (MSWD) for this 'error chron' is significantly large (958) and hence the age produced cannot be considered an absolute age for initiation of the Rb-Sr isotope system. It does still however indicate mobility of Rb and Sr during or just before the Delamerian Orogeny.

Poodla, other Olary Domain intrusives and metasediment εNd data are plotted in Figure 13. The Poodla samples were chosen to span a range from least altered ('primary' εNd = –3.3) to partially Na-Ca altered (εNd = –5.4) and most altered (εNd = –9.0). As the most altered sample is ~90% albite, the initial Nd-isotopic ratio is considered to approach the isotopic composition of the alteration fluid. As indicated in Figure 13, this ratio is below that of all the intrusives and most similar to the plotted meta-sediment data.

4. INTERPRETATION OF RESULTS

4.1 Age and Genesis of the Poodla Granite

The foliation in the granite indicates that it intruded and crystallised at least prior to OD4 and also likely prior to OD3 folding. Enclaves chosen for investigation were psammo-pelitic and pelitic in composition. Thus if any pre-intrusion fabric-producing event occurred it would be expected to be present in the chosen enclaves. As no pre-intrusion foliation was found it indicates the granite intruded prior to the Olarian orogeny.

Dating of Antro by Page et al. (2003) corroborates a Pb/Pb zircon evaporation date obtained by Freeman (1995) of 1679±13 Ma. Inspection of incompatible element distribution (Figure 7a) indicates Poodla is most similar to Antro. Samples (PD1f and PD47) analysed from the Poodla sampling site for the dating of Page et al. (2003) indicate the material dated to be part of the granite body and not a large allochthonous igneous enclave, as thought possible by those workers. This indicates that the date obtained is either correct or an inherited crystallisation age of an igneous source rock (zircons are reported to be unequivocally magmatic, Page pers. comm., 2003).

Consideration of the present data indicates the crystallisation age of Poodla Granite is similar to that of the Basso Suite age or, more likely, temporally related to Antro. The previous absolute age of 1629 ± 12 Ma (Cook et al., 1994) is thought to be a mixed age as a result of thermal perturbation associated with later tectonothermal events.

The initial εNd (Figure 13) value of Poodla (-3.2) is significantly lower than those obtained at Antro (-0.9 – -1.8, Freeman (1995)) but still greater than those typical of the Bimbowrie Supersuite (-4.7 – -6.7, Benton, 1994; Stoian, unpub. data). If Poodla and Antro are a similar age, this indicates Poodla is likely derived from a source similar to Antro but has undergone significantly more crustal assimilation. Calculations, involving meta-sediment (-4 to -7.3, Barovich, 2003; Benton, 1994) and depleted mantle (~4.9) εNd at the time, indicate approximately 7-20% crustal assimilation with a depleted mantle source. Equivalent calculations indicate Antro had less than 5% crustal assimilation.

4.2 Alteration

As reported, four styles of alteration are recorded by Poodla granite and in the immediate vicinity.

Within the granite potassic alteration pre-dates the pervasive Na-Ca alteration as evidenced by alteration of biotite veining produced by the earlier event. Due to a lack of unaltered granite, chemical characterisation of the early potassic alteration is not possible, and hence analysis of all later events, despite modelling of magmatic trends, may be affected by this event.

Na-Ca altered psammitic metasediments have been folded during OD3, hence pervasive Na-Ca alteration pre-dates this event. εNd(T) ratios progressively decrease (Table 7)

with increasing intensity of pervasive Na-Ca alteration. Intense alteration (~90% albite) displays a εNd(T) value of –9.01, similar to the basinal sediments at the time. This suggests that the fluids, and their dissolved components, responsible for the pervasive Na-Ca alteration were sourced from the lower Willyama Supergroup sediments. In light of this evidence, the potassic alteration may be an expression of the Na-Ca alteration fluids in the meta-sediments carrying excess K into the granite. This is then followed by the Na-rich fluids, which have reached a meta-stable equilibrium with the sediments (ie. no longer deposit significant Na and remove K), passing into the granite and resulting in Na-Ca alteration.

Field evidence and fluid inclusions studies indicate that the fracture-controlled sodic and Ca-Na-Si alteration and actinolite/clinopyroxene breccia are a single event caused by evolving fluids.

Evidence of Ca enrichment during the Ca-Na-Si event is demonstrated particularly well in the surrounding meta-sediments by the formation of epidote and actinolite (Figure 4d). Fe loss of up to 4.5% is comparable to one pervasive Na-Ca alteration sample, PD17, which is also expected to have fluid influence from nearby late pegmatite/quartz veining. The variation in Ca-Na-Si sample chemistry (minor/no Ca enrichment) can be explained by considering the influence of fracture- controlled sodic alteration. If the samples PD41a and PD41b experienced intense sodic alteration along the same fracture-pathway (as is thought likely in many cases), the samples would inherit this pre-existing alteration chemistry. This would then indicate that fracture-controlled sodic alteration caused near complete removal of Ca from the rock, Na enrichment and K depletion.

Homogenisation temperatures and composition of fluid inclusions raise a number of pertinent questions and correlations. Homogenisation temperatures for three-phase inclusions show interesting variation. Those of the Ca-Na-Si alteration have solid dissolution at 140-150˚C compared to solid dissolution in fracture-sodic fluids resulting in homogenisation at 245-290˚C. These higher dissolution temperatures may be indicative of higher concentrations of Na in the fluid, as the solid phase is likely to be NaCl.

Variation of homogenisation temperatures of coeval fluid inclusions indicates either a changing pressure and/or temperature at the time of formation. Figure 14a and 14b display possible relationships between the high and low salinity fluids involved in the fracture-controlled sodic and Ca-Na-Si alteration. In both cases the low salinity fluids would form either at higher pressure or lower temperature than the high salinity fluids. It is suggested that variation of pressure created the variation in trapping conditions, with relatively minor temperature variation. This indicates that the low salinity fluids, which, at the time, were over-pressured, initially infiltrated the system causing significant fracturing and forming the inclusion hosting quartz. Continuing influx of the low salinity fluid and influx of the high salinity fluid followed. Variation in fluid pressure of up to 1.5 kbar results in the difference of homogenisation temperatures between the two fluids. Fluid pressure fluctuations are demonstrated elsewhere in the domain as the cause of brecciation (Clark and James, 2003).

Composition of the fluids causing fracture-controlled sodic and Ca-Na-Si alteration correlate particularly well with data from Kent et al. (2000) for fluid compositions associated with actinolite/clinopyroxene matrix breccias at Cathedral Rock. These breccias are similar to those found in the study area, also likely to be related to the fracture-controlled alteration. Kent et al. (2000) reported a low salinity two-phase composition (15-30 wt% NaCl equivalent) and a high salinity three-phase composition (30-40 wt% NaCl equivalent). Homogenisation temperatures ranged between 160-340˚C. T_h between the two studies differs, but not to the extent, especially when considering possible pressure differences, to which they could be considered unrelated. Kent et al. (2000) applied a pressure correction of 4-6 kbar resulting in estimated formation temperatures between 400-600˚C. This post-tectonic alteration was reported as a result of devolatisation during regional metamorphism. Based upon similarity of fluid inclusions and timing relative to the orogen, the same is suggested for the fracture-controlled sodic, Ca-Na-Si and actinolite/clinopyroxene breccia event within the study area. Devolatisation after peak metamorphic (peak pressure) conditions commonly occurs on a clockwise P-T path (Yardley, 1997). Such a path has recently been demonstrated for the Olarian Orogeny (Hand et al., 2003; Swapp and Frost, 2003) in opposition to the previously described anti-clockwise P-T path of Clarke et al. (1987).

Biotite-matrix breccia within the area cannot be linked definitively to either of the two alteration/fluid movement events. It is known from field relations to have occurred prior to the fracture-controlled alteration and actinolite/clinopyroxene breccia event. This does not mean, however, it is not also due to devolatisation during regional metamorphism.

Fluid movement within the area also occurred during or shortly before the Delamarian Orogeny. Homogenisation of the Sr/Rb isotope system indicates this event was significant. It may be the case that production of a fine-grained mineral thought to be a clay mineral (~48 wt% SiO_2, ~30 wt% Al_2O_3, ~6 wt% $Fe_2O_{3(T)}$, ~6.3 wt% K_2O and ~2 wt% MgO), otherwise attributed to weathering, occurred during this Palaeozoic event.

The above interpretation suggests two major alteration events occurred at Poodla, pervasive potassic/Na-Ca and the later fracture-controlled sodic and Ca-Na-Si event. This has been followed by Delamerian movement of fluids, homogenising the Sr/Rb isotope system. The biotite-matrix breccia may be related to one of the first two events.

5. REGIONAL CU-AU IMPLICATIONS

5.1 Timing and Fluid Movement Mechanisms of Cu-Au mineralisation

Recent geochronology (Re-Os, Skirrow et al., 1999) indicates that Cu-Au mineralisation in the Olary Domain occurred in the 1632-1612 Ma interval, a pre-Olarian timing. This mineralisation has been subsequently modified by later addition and mobilisation during the Olarian and Delamarian orogenies (Conor, 2003). In a more recent paper Skirrow (2003) indicated that he now believes all mineralisation to be syn-tectonic and cites a 1% error inherent in Re-Os dating as reason to doubt the earlier ages. Discussions of hydrothermal mineralisation settings inevitably focus on the physical conditions leading to instigation of fluid flux. If these mineralising event ages prove reliable, it now appears there is no magmatic event synchronous with mineralisation. Therefore movement mechanisms other than direct magmatic thermal input must be involved. A change from extensional to compressional tectonic regimes marks the onset of the Olarian Orogeny and may be a driving mechanism for instigation of intrabasinal fluid cycling (Morrow, 1998). Similar regional fluid vectors are described for the Adelaide Geosyncline by Foden et al. (2001). In that particular instance fluid movement was indicated by homogeneity of sediment Sr isotope ratios and the interruption of this regime correlated to renewed rifting. Importantly it was this fluid flow that was suggested as the mineralising fluid for Cu deposits (eg. Kapunda and Mt Gunson) along the basin's western margin.

5.2 Regional Cu-Au mineralisation and alteration fluids

Examination of Au and Cu concentrations within the Poodla Granite indicates much with regard to their mobilisation during alteration. Depletion of Au within Poodla with respect to typical Poodla type granite and other regional granite values (Figure 15) indicates mobility of Au associated with the pervasive Na-Ca and/or potassic alteration. Cu on the other hand tends to be enriched in the granite (Figure 8h) but at relatively insignificant levels. This suggests that the pervasive Na-Ca alteration fluids have the ability to mobilise Cu and Au, and within the study area have deposited and removed these metals, respectively.

The majority of known Cu-Au mineralisation in the Olary Domain occurs along or near the regional redox and permeability boundary represented by the Bimba Formation (Leyh and Conor, 2000). This suggests that fluids moving up through the stratigraphic column reach this level and are halted in their progress due to a lack of permeability at and above the Bimba Formation and/or deposit Cu-Au due to the change in oxidation conditions. If fluids were being trapped at this level, consideration of not only the fluids involved in alteration, but also a predicted evolution of the fluids with regard to element mobility at the time of alteration is necessary for regional application to mineralisation models. Early pervasive Na-Ca fluids at Poodla are indicated to be potential carriers of Cu and Au. This suggests the pervasive Na-Ca alteration fluid seen at Poodla may be the early sodic alteration seen at Cu-Au prospects or may evolve into the later, main stage alteration fluids (ie. Fe-Ca-K or K ± Na fluids at Kalkaroo, 1616-1612Ma, Skirrow et al., 2000)

6. CONCLUSION

The Poodla Granite is considered likely to have crystallised at a similar age to the Antro tonalite (~1679 Ma) or possibly as part of the Basso Suite. A significant consequence of either age is that Poodla, or any other I-type granite, had no direct thermal input into Cu-Au mineralisation in the Olary Domain. This requires either a different age of mineralisation than previously reported or a model similar to the basin fluid circulation as suggested in this work.

Two main Proterozoic fluid movement/alteration events exist in the study area, with a later Palaeozoic event indicated by Sr isotopes. The first of the alteration events, potassic and pervasive Na-Ca, has mobilised Cu and Au with the possible potential of transporting them to sites suitable for mineralisation. Sm/Nd isotopes indicate this fluid is sourced from the Willyama Supergroup sediments. The second event is linked to that described by Kent et al. (2000), a devolatisation of the Willyama Supergroup due to metamorphism.

Such widespread fluid movement with the potential for Cu-Au mineralisation would suggest significant Cu-Au mineralisation exists undiscovered in the Olary Domain.

ACKNOWLEDGEMENTS

Funds for this research were contributed by the Curnamona Team, PIRSA and Adelaide University.

I would like to thank my supervisors Andreas Schmidt-Mumm and John Foden.
Colin Conor is thanked for his regional knowledge and discussions and Christopher Clark for his “guidance”.

Karin Barovich and Martin Hand for helpful discussion, with special thanks to Karin for her insightful reviews of the manuscript. John Stanley and David Bruce, Adelaide University, are also thanked for their assistance in sample preparation and running of the XRF and TIMS.

Thankyou to family and friends.
Shane Johansen, and all others involved in inspiration.

REFERENCES

ASHLEY, P.M., COOK, N.D.J., & FANNING, C.M., 1996. Geochemistry and age of metamorphosed felsic igneous rocks with A-type affinities in the Willyama Supergroup, Olary Block, South Australia and implications for mineral exploration. Lithos **38**: 167-184.

ASHLEY, P. M., LAWIE, D. C., CONOR, C. H. H. & PLIMER, I. R., 1997. Geology of the Olary Domain, Curnamona Province, South Australia and field guide to 1997 excursion stops. Department of Mines and Energy South Australia, Report Book 97/17.

ASHLEY, P. M., CONOR, C. H. H. & SKIRROW, R. G., 1998. Geology of the Olary Domain, Curnamona Province, South Australia. Field Guidebook to Broke Hill Exploration Initiative Excursion 13-15 October 1998, Primary Industries and Resources South Australia.

BAROVICH, K. M., CONOR, C. & FODEN, J., 2002. Geochemical and Nd isotope constraints on provenance of the Willyama Supergroup, South Australia, and comparisons to the Mt Isa Inlier. Geological Society of Australia, Abstracts **67**, 155.

BAROVICH, K. M., 2003. Geochemical and Nd isotopic evidence for sedimentary source changes in the Willyama Basin, Curnamona Province. In: Peljo, M., comp.,

2003. Broken Hill Exploration Initiative: Abstracts from the July 2003 conference. Geoscience Australia Record 2003/13, pp. 3-5.

BENTON, R.Y., 1994. A petrological, geochemical and isotopic investigation of granitoids from the Olary Province of South Australia. BSc (Hons) thesis, University of Adelaide (unpub.).

BIERLEIN,F. P., 1995. Rare-earth element geochemistry of clastic and chemical metasedimentary rocks associated with hydrothermal sulphide mineralisation in the Olary Block, South Australia. Chemical Geology **122**, 1-4, 77-98.

CLARK, C. & JAMES, P., 2003. Hydrothermal brecciation due to fluid pressure fluctuations: examples from the Olary Domain, South Australia. Tectonophysics **366**, 187-206.

CLARKE, G., BURG, J. & WILSON, C., 1986. Stratigraphic and Structural constraints on the Proterozoic tectonic history of the Olary Block, South Australia. Precambrian Research **34**, 107-137.

CLARKE, G., GUIRAUD, M., WILSON, C. & BURG, J., 1987. Metamorphism in the Olary Block, South Australia; compression with cooling in a Proterozoic fold belt. Journal of Metamorphic Geology **5**, 291-306.

CONOR, C. H. H, 2000. Definition of major sedimentary and igneous units of the Olary domain, Curnamona Province. MESA Journal **19**, 51-56.

CONOR, C. H. H, 2003. Geology of the Olary Domain, Curnamona Province, South Australia. Broken Hill Exploration Initiative, 2003, Field Excursion Guidebook.

COOK, N. D. J., FANNING, C. M. & ASHLEY, P. M., 1994. New geochronological results from the Willyama Supergroup, Olary Block, South Australia. *In:* Australian Research on Ore Genesis Symposium. Adelaide, Australian Mineral Foundation 19.1-19.5.

ELBURG, M. A., BONS, P. D., FODEN, J. & BRUGGER, J., 2003. A newly defined Late Ordovician magmatic-thermal event in the Mt Painter Province, northern Flinders Ranges, South Australia. Australian Journal of Earth Sciences **50**, 611-631.

FERRIS, G., SCHWARZ, M. & HEITHERSAY, P., 2002. The geological framework, distribution and controls of Fe-oxide related alteration, and Cu-Au mineralisation in the Gawler Craton, South Australia: Part 1: Geological and tectonic framework. In: Porter, T. M. (Ed.), Hydrothermal Iron Oxide Copper-Gold & Related Deposits: A Global Perspective, vol. 2, PGC Publishing, pp. 7-22, Adelaide.

FLINT, D. & PARKER, A., 1993. Willyama Inliers. In: Drexel, J., Preiss, W., Parker, A. (Eds.), The Geology of South Australia. Geological Survey of South Australia, Bulletin, vol. 54, pp. 82-93. Adelaide.

FODEN, J., BAROVICH, K., JANE, M. & O'HALLORAN, G., 2001. Sr-isotopic evidence for Late Neoproterozoic rifting in the Adelaide Geosyncline at 586Ma: implications for a Cu ore forming fluid. Precambrian Research **106**, 291-308.

FREEMAN, H., 1995. A Geochemical and isotopic study of mafic and intermediate rocks in the Olary Province, South Australia – Magma Series Discrimination and Geochronological framework. BSc (Hons) thesis, University of Adelaide (unpub.).

GRANT, J. A., 1986. The Isocon Diagram- A simple Solution to Gresens' Equation for metasomatic Alteration. Economic Geology **81**, 1976-1982.

GRESEN, R. L., 1967. Composition-Volume Relationships in Metasomatism. Chemical Geology **2**, 47-55.

HAND, M., RUTHERFORD, L. & BAROVICH, K., 2003. Garnet Sm-Nd age constraints on the timing of tectonism in the southwestern Curnamona Province: Implications for existing models and correlations. In: Peljo, M., comp., 2003. Broken Hill Exploration Initiative: Abstracts from the July 2003 conference. Geoscience Australia Record 2003/13, pp. 65-68.

HILL, P., 1995. Geology of the Tonga Hill, Poodla Hill, Telechie Valley area, Bimbowrie, Olary, South Australia. BSc (Hons) thesis, University of New England (unpub.).

JOHNSON, J. P. & MCCULLOCH, M. T., 1995. Sources of mineralising fluids for the Olympic Dam deposit (South Australia): Sm-Nd isotopic constraints. Chemical Geology **121**, 177-199.

KENT, A. J. R., ASHLEY, P. M. & FANNING, C. M., 2000. Metasomatic alteration associated with regional metamorphism: an example from the Willyama Supergroup, South Australia. Lithos **54**, 33-62.

LEYH, W. R. & CONOR, C. H. H., 2000. Stratigraphically controlled metallogenic zonation associated with the regional redox boundary of the Willyama Supergroup; economic implications for the southern Curnamona Province. MESA Journal **16**, 39-47.

MARK, G., 1999. Petrogenesis of Mesoproterozoic K-rich granitoids, southern Mt Angelay igneous complex, Cloncurry district, northwest Queensland. Australian Journal of Earth Sciences **46**, 933-949.

MORROW, D., 1998. Regional subsurface dolomitisation: models and constraints. Geoscience Canada **25**, 57-70.

NOBLE, M. P., FRY, K., BETTS, P. G., FORBES, C. & LISTER, G. S., 2003. High Temperature Shear zones of the Curnamona Province. In: Peljo, M., comp., 2003. Broken Hill Exploration Initiative: Abstracts from the July 2003 conference. Geoscience Australia Record 2003/13, pp. 120-121.

PAGE, R.W., STEVENS, B. P. J., GIBSON, G. M. & CONOR C. H. H., 2000. Geochronology of the Willyama Supergroup rocks between Olary and Broken Hill, and a comparison to northern Australia. In: Peljo, M. (Ed.), Broken Hill Exploration Initiative: abstracts of papers presented at the May 2000, conference in Broken Hill. AGSO Record, 2000/10, pp. 72-75.

PAGE, R., STEVENS, B., CONOR, C., PREISS, W., CROOKS, A., ROBERTSON, S., GIBSON, G. & FOUDOULIS, C., 2003. SHRIMP U-Pb Geochronology in the Curnamona Province: Improving the framework for mineral exploration. In: Peljo, M., comp., 2003. Broken Hill Exploration Initiative: Abstracts from the July 2003 conference. Geoscience Australia Record 2003/13, pp. 122-125.

PEARCE, J. A., HARRIS, N. B. W. & TINDLE, A.G., 1984. Trace Element discrimination diagrams for the tectonic interpretation of granitic rocks. Journal of Petrology **25**, 956-983.

POLLARD, P. J., MARK, G. & MITCHELL, L. C., 1998. Geochemistry of the post-1540 Ma granites in the Cloncurry district, northwest Queensland. Economic Geology **93**, 1330-1344.

RAETZ, M., KRABBENDAM, M., DONAGHY, A. G., 2002. Compilation of U-Pb zircon data from the Willyama Supergroup, Broken Hill region, Australia; evidence for three tectonostratigraphic successions and four magmatic events? Australian Journal of Earth Sciences. **49**, 965-983.

ROBERTSON, R. S., PREISS, W. V., CROOKS, A. F., HILL, P. W. & SHEARD, M. J., 1998. Review of the Proterozoic geology and mineral potential of the Curnamona Province in South Australia. AGSO Journal of Australian Geology and Geophysics **17**, 169-182.

ROEDDER, E., 1984. Fluid Inclusions. Reviews in Mineralogy, 12. Mineralogical Society of America.

SKIRROW, R. G. & ASHLEY, P. M., 1998. Cu-Au mineral systems and regional alteration, Curnamona Craton. AGSO record **1998/25,** 104-108.

SKIRROW, R. G., MAAS, R. & ASHLEY, P. M., 1999. New age constraints for Cu-Au (-Mo) mineralisation and regional alteration in the Olary-Broken Hill region. AGSO Research Newsletter **31**, 22-25.

SKIRROW, R.G., ASHLEY, P.M., MCNAUGHTON, N.J., & SUZUKI, K., 2000. Time-space framework of the Cu-Au(-Mo) and regional alteration systems in the Curnamona Province [abs.]: Broken Hill Exploration Initiative, May 2000, Australian Geological Survey Organisation, Record 2000/10, p. 83-86.

SKIRROW, R. G., 2003. Fe-oxide Cu-Au deposits: Potential of the Curnamona Province in an Australian and Global Context. In: Peljo, M., comp., 2003. Broken Hill Exploration Initiative: Abstracts from the July 2003 conference. Geoscience Australia Record 2003/13, pp. 158-161.

SUN, S. S. & MCDONOUGH, W. F., 1989. Chemical and isotopic systematics of ocean basalts: implications for mantle composition and processes. In: Sauders, A. D. & Norry, M. J. (eds.). Magmatism in the Ocean Basins. Geological Society of London , Special Publication 42, 313-345.

SWAPP, S. M. & FROST, R. B., 2003. Evidence for high-pressure metamorphism in the granulites of the Broken Hill area. In: Peljo, M., comp., 2003. Broken Hill Exploration Initiative: Abstracts from the July 2003 conference. Geoscience Australia Record 2003/13, pp. 174-175.

VAN DEN KERKHOF, A. M. & HEIN, U. F., 2001. Fluid inclusion petrography. Lithos **55**, 27-47.

WHALEN, J. B., CURRIE, K. L. & CHAPPELL, B. W., 1987. A-type granites: geochemical characteristics, discrimination and petrogenesis. Contributions to Mineralogy and Petrology **95**, 407-419.

WYBORN, L., 1998. Younger ca 1500 Ma granites of the Williams and Naraku batholiths, Cloncurry District, eastern Mt Isa Inlier; geochemistry, origin, metallogenic significance and exploration indicators. In: Pollard-P-J (ed.) Geological framework and mineralisation in the Mt Isa Eastern Succession, Northwest Queensland. Australian Journal of Earth Sciences **45,** 3, 397-411.

YARDLEY, B. W. D., 1997. The evolution of fluids through the metamorphic cycle. In: Yardley, B. W. D. & Jamveit, V. (eds.), 1997. Fluid flow and transport in rocks. Chapman & Hall, London. pp. 99-122.

FIGURE CAPTIONS

Figure 1 – Simplified regional geology and location of Poodla Granite.

Figure 2 – Olary Domain stratigraphy and levels of emplacement of Intrusive suites (after Conor, 2003).

Figure 3 – Geological outcrop map of study area.

Figure 4 – a) Stereonet plot of OF3, OF4 and DF fold hinge orientations.

b) Contoured stereonet plot of S_0/S_1 poles from the study area. Demonstrates pre-dominant NE/SW alignment of structure due to OD3. Majority of variation occurs in the 'pressure shadow' directly to the north of the granite.

c) Stereonet plot of mineral elongations demonstrating OD4 plane of shear.

d) Stereonet plot of fluid inclusion planes in quartz associated with Ca-Na-Si alteration. Data obtained does not provide enough information to accurately determine the palaeo-stress field.

(All stereonets are lower hemisphere, equal area projection).

Figure 5 – a) Photomicrograph of biotite veining in granite (altered to Mg-rich composition). (Plane polarised light, 100x magnification).

b) Photomicrograph of pervasive Na-Ca altered granite. Progressive albitisation is seen from its lower contact with K-feldspar to the top of the image. Inclusions in albite are altered biotite. (X-Polars, 100x magnification)

c) Quartz/albite filled fractures with sodic alteration fringe. Cross-cutting earlier quartz veining.

d) Actinolite produced by Ca-Na-Si alteration in previously albitised meta-sediments. Actinolite is dark coloured veining.

Figure 6 – a) Primitive mantle normalised incompatible element plot of least-altered Poodla, Antro (Benton, 1994), South Willow (Freeman, 1995), typical Basso (Benton, 1994; Stoian, unpub. data) and Mt Angelay intrusives (Mark, 1999).

b) Primitive mantle normalised incompatible element plot of selected Poodla Granite samples. (Normalisation factors: Sun and McDonough, 1989).

Figure 7 – a) Nb/Y Tectonic classification diagram (Pearce et al., 1984). Samples PD1f and PD47.

b) mol. Al_2O_3 / (Na_2O+K_2O) *vs* Al_2O_3 / (CaO+Na_2O+K_2O). Note: variation due to progressive alteration.

c) S-, I-, A-type discrimination diagram (after Whalen et al., 1987). Samples PD1f and PD47.

Figure 8– a-g) Harker diagrams of actual major element concentrations and modelled fractionation trends of natural analogue.

h) Cu/SiO_2 plot of Poodla also showing comparative magmatic trend of Mt Angelay Igneous Complex.

Figure 9 – Example isocon diagram. Data plotted is a pervasive Na-Ca sample, PD13. Al_2O_3 and TiO_2. Elements plotting above isocon show mass gain, elements plotting below show a mass loss during alteration.

Figure 10 –Increase/decrease (wt%) of major elements due to alteration.

Figure 11 – a) 2-phase, low salinity fluid inclusions associated with Ca-Na-Si alteration.

b) 3-phase, high salinity fluid inclusions associated with Ca-Na-Si alteration.

Figure 12 – Sr/Rb 'isochron'.

Figure 13 – εNd/age plot: Olary intrusives and metasediment data (after Stewart and Foden, unpub. data).

Figure 14 – a) Liquidi and iso-T_h lines for fluid inclusions associated with fracture-controlled sodic alteration (after Bodnar and Vityk, 1994). Low salinity iso-T_h lines are drawn for a salinity of 20 wt% NaCl. High salinity liquidi and iso-T_h is drawn for salinities of approximately 35 and 38 wt% NaCl

(based upon solid phase dissolution temperature). Shaded field represents possible formation conditions and demonstrates pressure decrease for formation of high salinity fluids at constant temperature.

b) Liquidi and iso-T_h lines for fluid inclusions associated with Ca-Na-Si alteration (after Bodnar and Vityk, 1994). Low salinity iso-T_h lines are drawn for a salinity of 20 wt% NaCl. High salinity liquidi and iso-T_h is drawn for salinities of approximately 30 wt% NaCl (solid phase dissolution at 158°C). Shaded field represents possible formation conditions and demonstrates pressure decrease for formation of high salinity fluids at constant temperature.

Figure 15 – Au values of regional intrusive suites (regional data from Stewart and Foden, unpub. data).

TABLES

Table 1 – Regional Tectonic Summary (after Conor, 2003)

Age	Tectonic Event	Abb. #	Characteristics
	Onset of Rifting		
	Willyama Supergroup Deposition		
1715-1707 & ~1685	Coeval Volcanics and intrusives (Basso and Lady Louise)		
	?Pre-Orogenic		High T shear zones
~1600-1580	Faugh-a-ballagh(ian)	OD1	Macroscopic tight to isoclinal recumbent folds (S1)
	Mount Mulga(ian)	OD2	Moderate to shallow reclined axial planes Variable orientations (OF2)
	Cascade(ian)	OD3	Meso-Macroscopic, tight to open, upright to moderately northerly verging inclined folds. (OF3) Strong axial planar fabric (S3), locally intense crenulation
	Walter-Outalpa(ian)	OD4	W-E trending shear zones and W-E trending folds (OF4)
~1590-1580	Bimbowrie Suite Granitoids (S-type)		
~800	Rifting of Adelaide Geosyncline, Deposition of Adelaidean Sediments and associated mafic dykes (Gairdner Dyke Swarm)		
~500	Delamerian Orogeny	DD1	N-S trending folding, axial cleavage
		DD2	NE trend

Table 2 – Tectonothermal summary of study area

Intrusive and Orogenic events	Field Observations	Alteration	Characteristics of Fluid Movement
Intrusion of Poodla Granite			
Faugh-a-ballian (OD1)	Layer Parallel Foliation, layer parallel quartz veining	Pre-OD3 Na-Ca and K alteration	Pervasive i.e. grain boundaries
Mount Mulgaian (OD2)	Rare mesoscopic folds		
Cascadian (OD3)	Steeply plunging folding NE/SW Axial Planar cleavage Localised crenulation cleavage	Sodic & Ca-Na-Si alteration and actinolite/clinopyroxene breccia	Movement along fractures, large quartz veins (1m thick) and brecciation
Possible Walter-Outalpian (OD4)	Mylonite zone Shearing of granite E-W trending folding Crenulation cleavage development		
Delamerian	SSE plunging folding	Sr and/or Rb mobility	?Localised in and around shear zones?

Table 4 – Mineral Composition (Primary and Altered)

Oxides (wt%)	Primary Biotite	Altered Biotite	Primary Plagioclase	K – feldspar	Alteration Plagioclase (rim)	Alteration Plagioclase (core)
SiO_2	36.64	36.29	69.26	64.94	70.71	69.98
TiO_2	2.08	1.55	0.03	0.01	0.02	0.01
Al_2O_3	14.97	15.56	20.63	18.42	21.23	20.86
Fe_2O_3	1.31	3.45	0.10	0.14	0.02	0.0
FeO	20.28	17.59	0.00	0	0	0.0
MnO	0.13	0.22	0.01	0.09	0	0.0
MgO	12.19	12.17	0.01	0.01	0.04	0.0
CaO	0.02	0.01	0.60	0	0.3	0.25
Na_2O	0.08	0.04	13.21	0.57	13.95	13.48
K_2O	11.10	9.75	0.08	18.29	0.1	0.08
Total	**98.79**	**96.64**	**103.96**	**102.49**	**106.45**	**104.7**
No. of O	**11**	**11**	**8**	**8**	**8**	**8**
Cations						
Si	2.75	2.74	2.94	2.96	2.93	2.94
Ti	0.12	0.08	0.00	0	0.00	0.0
Al	1.32	1.38	1.03	0.99	1.03	1.03
Fe^{3+}	0.07	0.19	0.00	0.00	0.00	0.0
Fe^{2+}	1.27	1.11	0.00	0	0	0.0
Mn	0.01	0.01	0.00	0.00	0	0.0
Mg	1.36	1.37	0.00	0.00	0.00	0.0
Ca	0	0.00	0.03	0	0.01	0.01
Na	0.01	0.00	1.09	0.05	1.12	1.09
K	1.06	0.94	0.00	1.06	0.005	0.004
Total	**7.98**	**7.853**	**5.09**	**5.09**	**5.11**	**5.09**

Table 5 – Trace Element gain/loss during various styles and extents of alteration

	Sr	Rb	U	Th	Pb	Cu	Zn	Ni	Ba	Sc	Co	V	Ce	La	Cr
Na-Ca (ppm)	56	-153	-1	0	4	18	-15	1	-191	-2	4	-2	-15	-9	1
Na-Ca (%)	**229**	**-48**	**-12**	**-1**	**361**	**46**	**-46**	**10**	**-21**	**-11**	**10**	**-4**	**-13**	**-16**	**7**
Na-Ca (ppm) PD15	39	-318	-6	-22	2	-32	-32	-9	-899	-16	-17	-51	-118	-53	-9
Na-Ca (%) PD15	**161**	**-100**	**-89**	**-98**	**150**	**-84**	**-97**	**-75**	**-96**	**-96**	**-50**	**-91**	**-98**	**-100**	**-45**
Ca-Na-Si (ppm)	103	-298	-2	-9	2	-35	-24	-2	-786	0	2	16	-68	-34	12
Ca-Na-Si (%)	**420**	**-93**	**-23**	**-39**	**193**	**-91**	**-74**	**-19**	**-84**	**1**	**7**	**29**	**-56**	**-65**	**61**
Ca-Na-Si (ppm) PD41a & b	8	-306	-2	5	1	-32	-21	8	-903	-7	12	-4	-88	-46	15
Ca-Na-Si (%) PD41a & b	**33**	**-96**	**-31**	**20**	**80**	**-85**	**-65**	**63**	**-97**	**-42**	**35**	**-7**	**-73**	**-88**	**76**

Note: variation of 10% or less can be attributed to natural magmatic variation

Table 6 – Fluid Inclusion Analysis Results

Associated Alteration	**Fluid Inclusion Type**	**T_e (˚C)**	**T_m (˚C)**	**T_h(˚C)** Vapour homogenisation	**T_h (˚C)** Solid Dissolution	**Salinity** NaCl wt% equivalent
Fracture Sodic	2-phase (L+V)	-36.9 – -34.5	-25.7 – -22.0	150 – 185	-	24.0 – 26.4
	3-phase (L+V+S)	~ -56.0	-41.5 – -34.2	160 – 190	240 – 285	34.1 – 38.2
Ca-Na-Si	2-phase (L+V)	~-37.0	-25.2 – -18.2	170 – 209	-	21.3 – 26.1
	3-phase (L+V+S)	~-56.9	-43.8 – -38.9	217 – 246	~ 150 – 160	35.8 – 40.6

Table 7 – Sm/Nd and Rb/Sr isotope results

Sample	**PD-1F**	**PD-13**	**PD-15**	**PD-41a**
	Least altered	Na-Ca altered	Intense Na alteration (90% albite)	Ca-Na-Si alteration
Nd (ppm)	58.8	44.5	2.2	15.3
Sm (ppm)	10.9	8.8	0.5	5.7
$^{143}Nd/^{144}Nd$	0.511550	0.511540	0.511463	0.511741
$^{147}Sm/^{144}Nd$	0.111503	0.119916	0.129805	0.224144
εNd	-21.0	-21.4	-22.9	-17.5
Age (T) (Ma)	1629	1629	1629	1629
$^{143}Nd/^{144}Nd$ (T)	0.510365	0.510256	0.510072	0.50934
εNd (T)	**-3.3**	**-5.4**	**-9.0**	**-23.4**
T_{DM} (Ma)	2136	-	-	-
$^{87}Sr/^{86}Sr$	1.013075	0.783423	0.741437	0.748874
Sr ppm	29.5	126.8	63.9	30.9
Rb ppm	347.7	173.9	1.4	15.3
$^{87}Rb/^{86}Sr$	35.120	3.997	0.064	1.438
$^{87}Sr/^{86}Sr$(T=540 Ma)	**0.742741**	**0.752653**	**0.740948**	**0.737803**
$^{87}Sr/^{86}Sr$(T=1629 Ma)	0.191220	0.689879	0.739949	0.715215

FIGURES

Figure 1

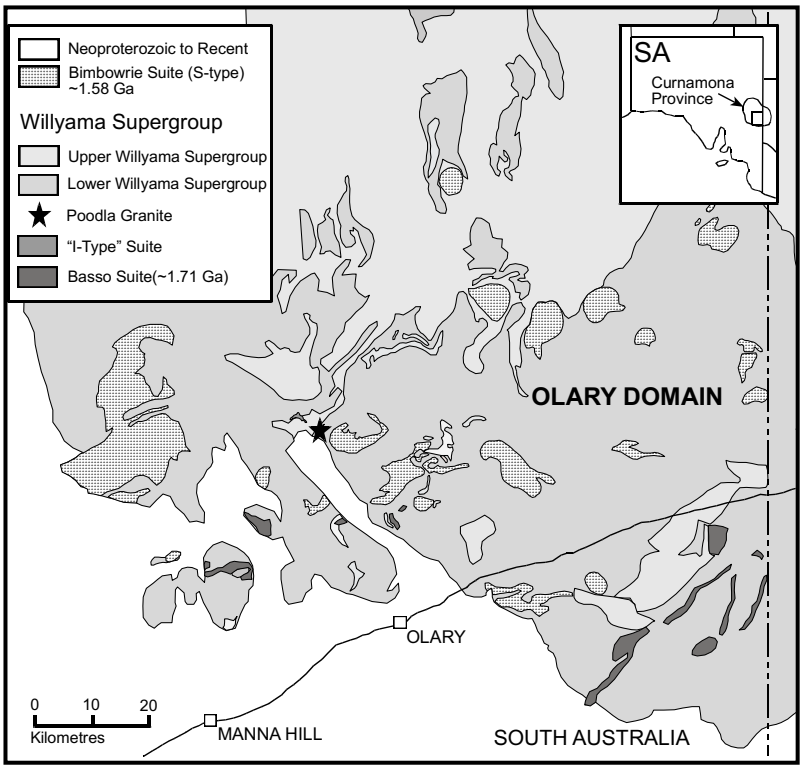

Figure 2

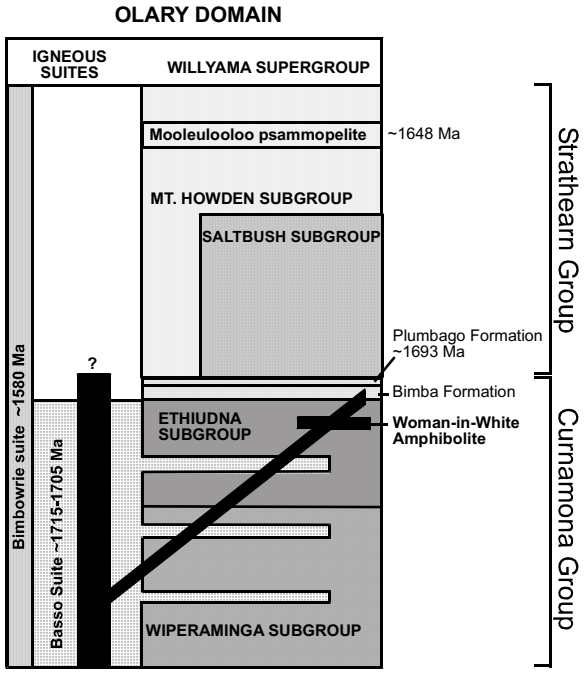
OLARY DOMAIN
IGNEOUS SUITES
WILLYAMA SUPERGROUP
Mooleulooloo psammopelite
~1648 Ma
MT. HOWDEN SUBGROUP
SALTBUSH SUBGROUP
Strathearn Group
Plumbago Formation
~1693 Ma
Bimba Formation
Woman-in-White Amphibolite
ETHIUDNA SUBGROUP
Curnamona Group
WIPERAMINGA SUBGROUP
Bimbowrie suite ~1580 Ma
Basso Suite ~1715-1705 Ma
?

Figure 3

Figure 4

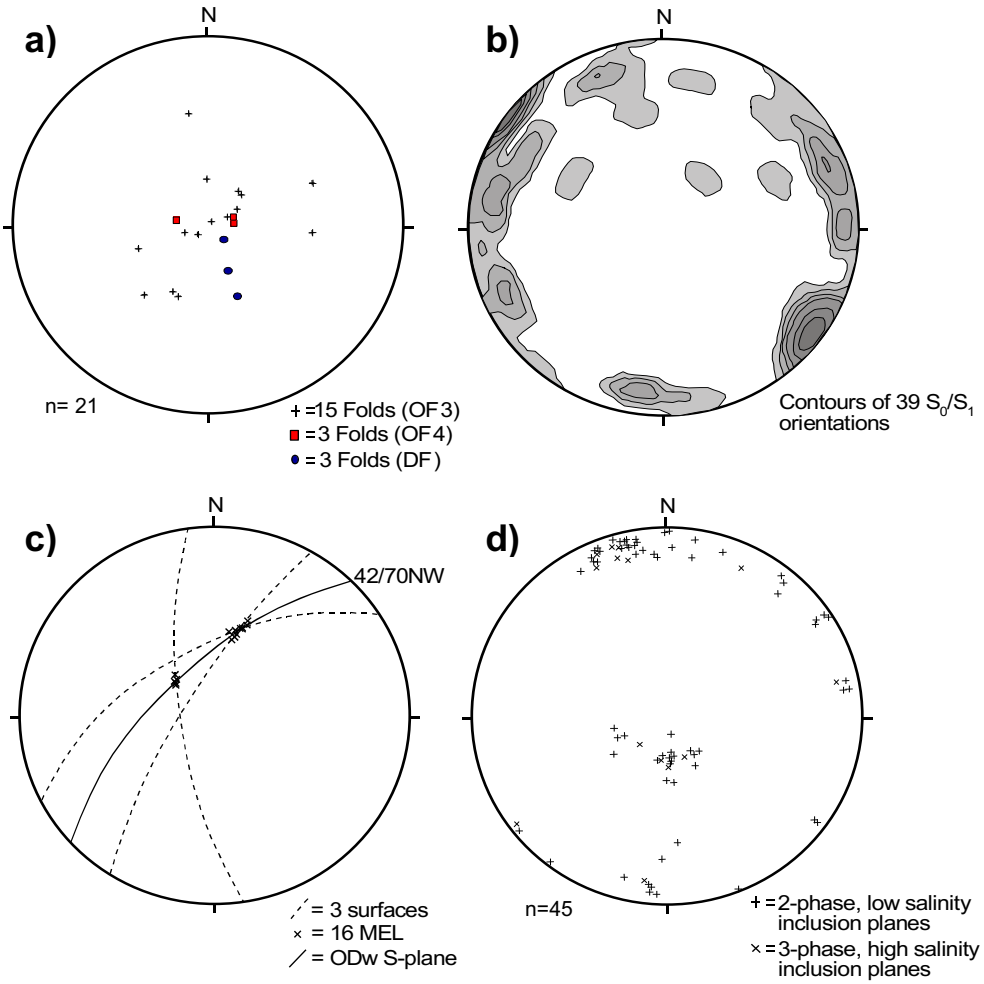
a)
N
n= 21
+ =15 Folds (OF3)
= 3 Folds (OF4)
= 3 Folds (DF)
b)
N
Contours of 39 S0/S1 orientations
c)
N
42/70NW
= 3 surfaces
× = 16 MEL
= ODw S-plane
d)
N
n=45
+ = 2-phase, low salinity inclusion planes
× = 3-phase, high salinity inclusion planes

Figure 5

Figure 6a

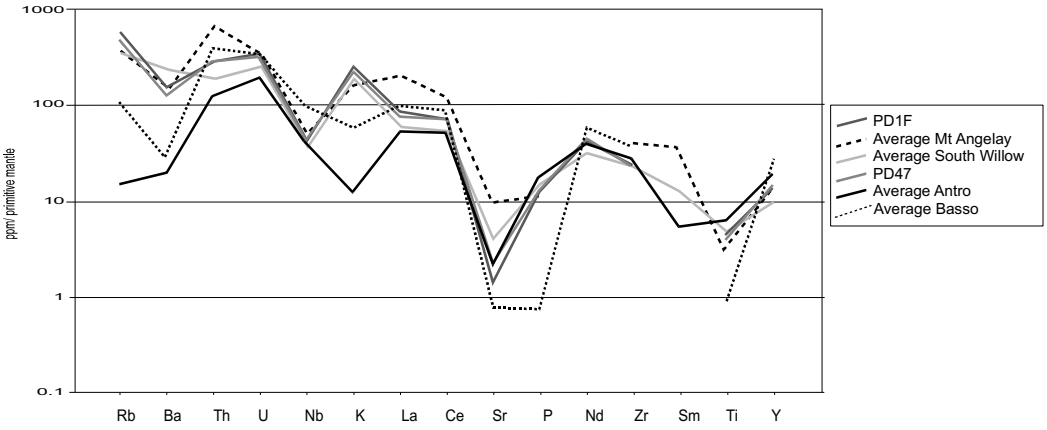
1000
100
10
1
0.1
ppm/ primitive mantle
Rb
Ba
Th
U
Nb
K
La
Ce
Sr
P
Nd
Zr
Sm
Ti
Y
PD1F
Average Mt Angelay
Average South Willow
PD47
Average Antro
Average Basso

Figure 6b

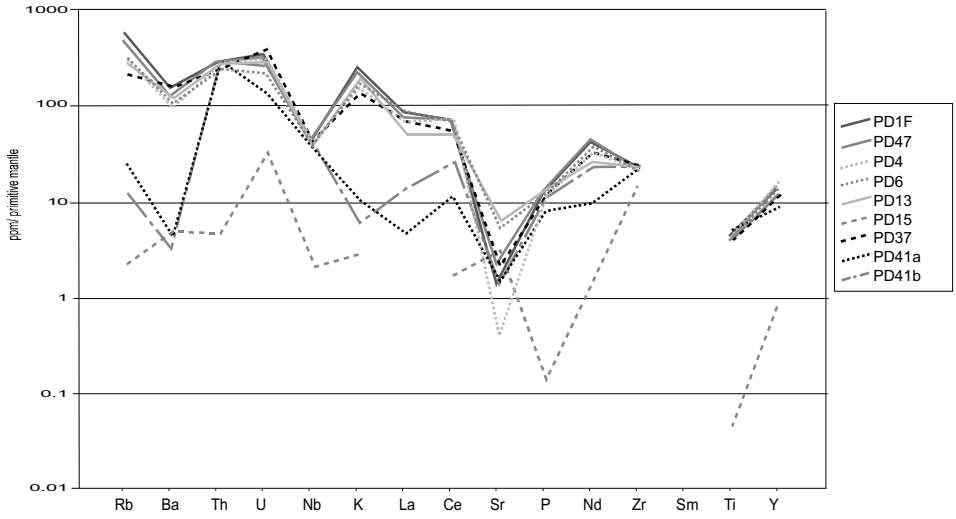
1000
100
10
1
0.1
0.01
ppm/ primitive mantle
Rb
Ba
Th
U
Nb
K
La
Ce
Sr
P
Nd
Zr
Sm
Ti
Y
PD1F
PD47
PD4
PD6
PD13
PD15
PD37
PD41a
PD41b

Figure 7a

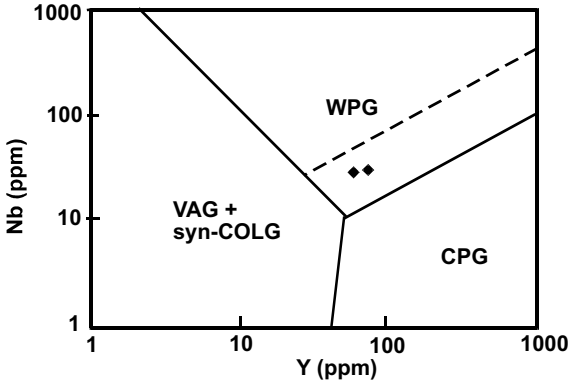

Figure 7b

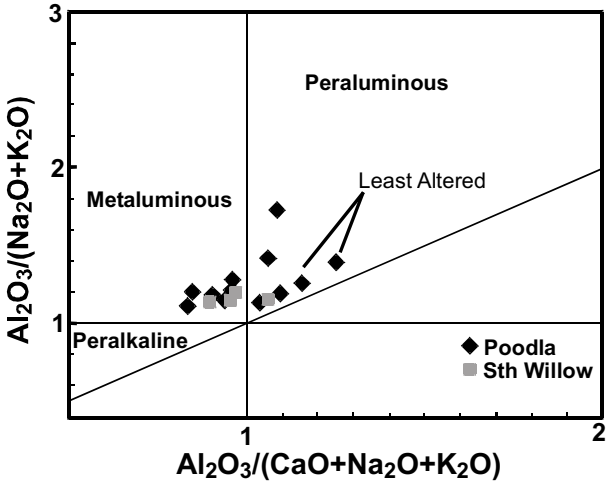
3
2
1
Peraluminous
Metaluminous
Least Altered
Peralkaline
Poodla
Sth Willow
1
2
Al2O3/(Na2O+K2O)
Al2O3/(CaO+Na2O+K2O)

Figure 7c

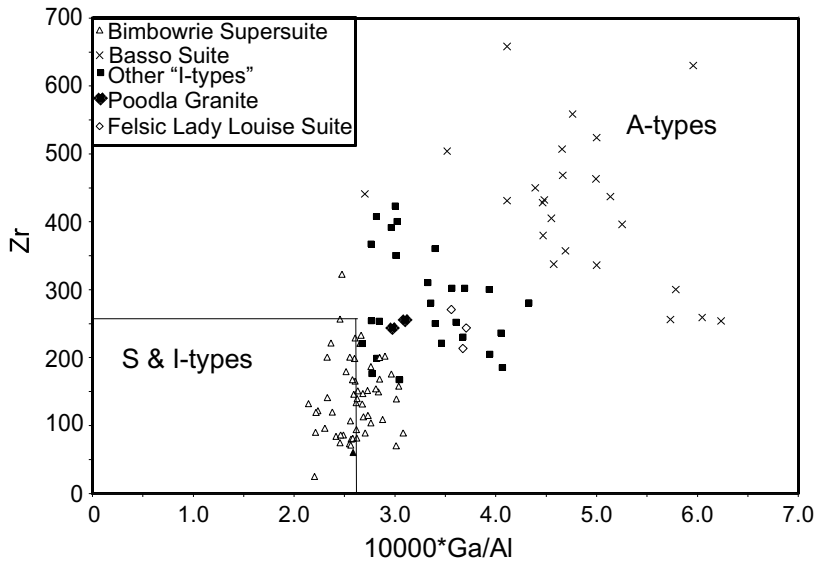
Bimbowrie Supersuite
Basso Suite
Other "I-types"
Poodla Granite
Felsic Lady Louise Suite
A-types
S & I-types
Zr
10000*Ga/Al
0
100
200
300
400
500
600
700
1.0
2.0
3.0
4.0
5.0
6.0
7.0

Figure 8

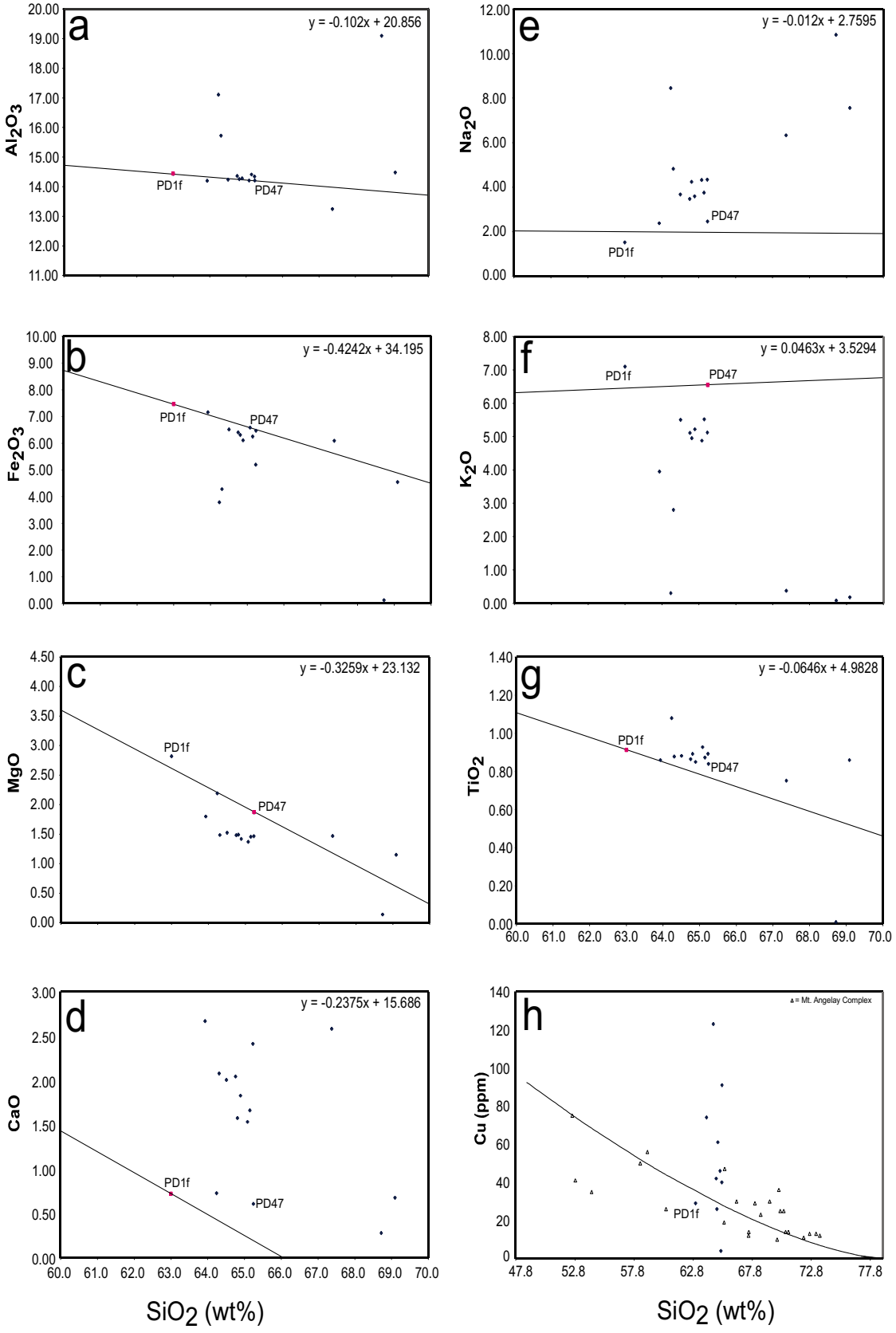
a
y = -0.102x + 20.856
Al2O3
PD1f
PD47
b
y = -0.4242x + 34.195
Fe2O3
PD1f
PD47
c
y = -0.3259x + 23.132
MgO
PD1f
PD47
d
y = -0.2375x + 15.686
CaO
PD1f
PD47
SiO2 (wt%)
e
y = -0.012x + 2.7595
Na2O
PD47
PD1f
f
y = 0.0463x + 3.5294
K2O
PD1f
PD47
g
y = -0.0646x + 4.9828
TiO2
PD1f
PD47
h
▲= Mt. Angelay Complex
Cu (ppm)
PD1f
SiO2 (wt%)

Figure 9

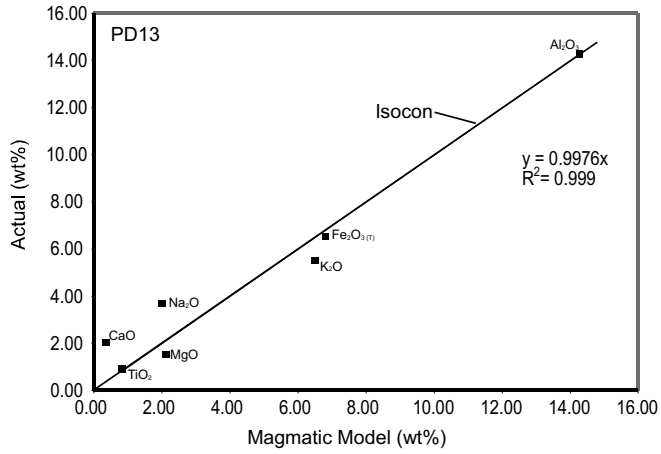
PD13
Isocon
y = 0.9976x
R2= 0.999
Al2O3
Fe2O3 (T)
K2O
Na2O
CaO
MgO
TiO2
Actual (wt%)
Magmatic Model (wt%)
0.00
2.00
4.00
6.00
8.00
10.00
12.00
14.00
16.00

Figure 10

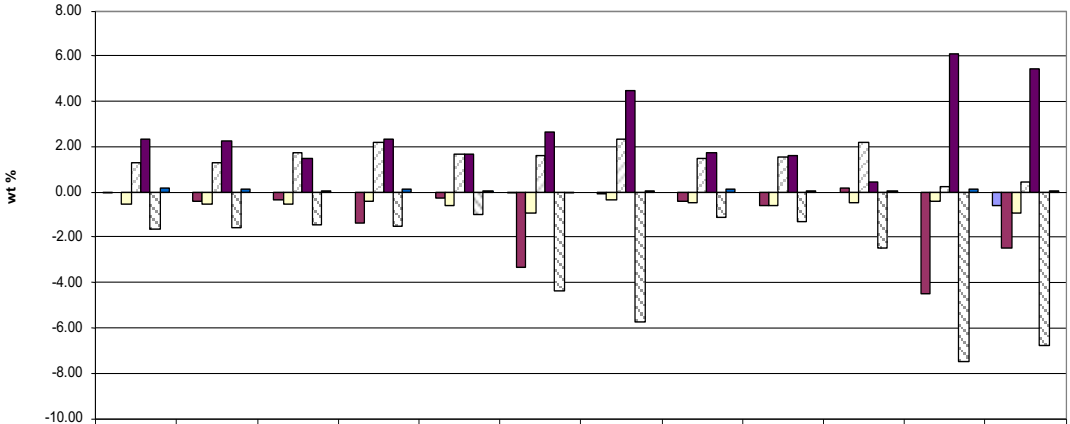

	PD4	PD5	PD6	PD12	PD13	PD17	PD20	PD22	PD14	PD37	PD41a	PD41b
Al2O3	-0.008	-0.005	-0.003	-0.0066	-0.004	0.002	-0.001	-0.005	-0.0028	-0.0004	-0.004	-0.612
Fe2O3T	-0.002	-0.399	-0.374	-1.3955	-0.301	-3.322	-0.073	-0.404	-0.5800	0.1506	-4.519	-2.475
MgO	-0.551	-0.521	-0.562	-0.4269	-0.580	-0.904	-0.346	-0.472	-0.5707	-0.4756	-0.437	-0.917
CaO	1.304	1.282	1.736	2.2183	1.641	1.626	2.351	1.445	1.5545	2.1721	0.216	0.416
Na2O	2.342	2.255	1.469	2.3425	1.691	2.637	4.487	1.745	1.6028	0.4064	6.070	5.459
K2O	-1.665	-1.586	-1.470	-1.4954	-0.996	-4.356	-5.715	-1.119	-1.3347	-2.4784	-7.481	-6.757
TiO2	0.149	0.094	0.059	0.1160	0.068	-0.033	0.022	0.087	0.0566	0.0151	0.083	0.028

Figure 11

Figure 12

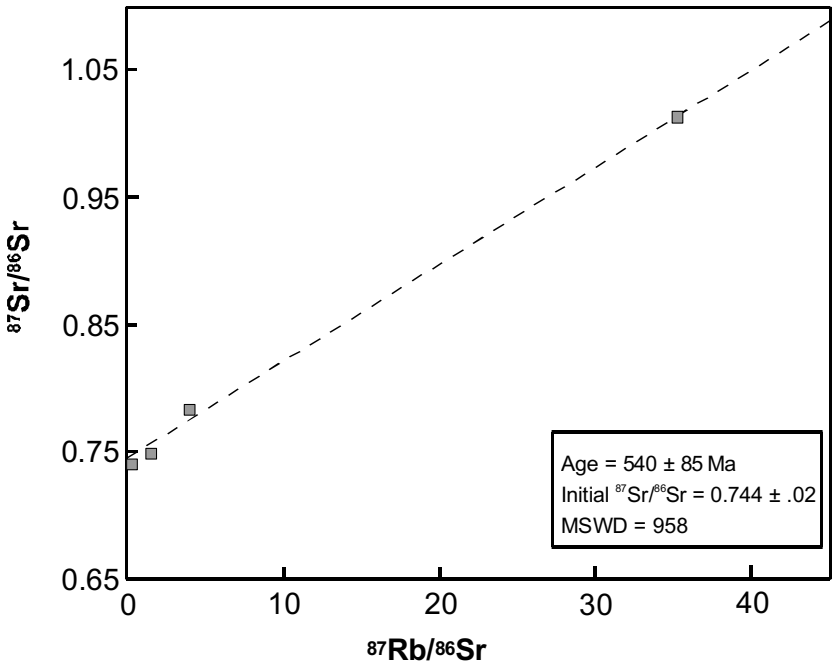
1.05
0.95
0.85
0.75
0.65
0
10
20
30
40
87Sr/86Sr
87Rb/86Sr
Age = 540 ± 85 Ma
Initial 87Sr/86Sr = 0.744 ± .02
MSWD = 958

Figure 13

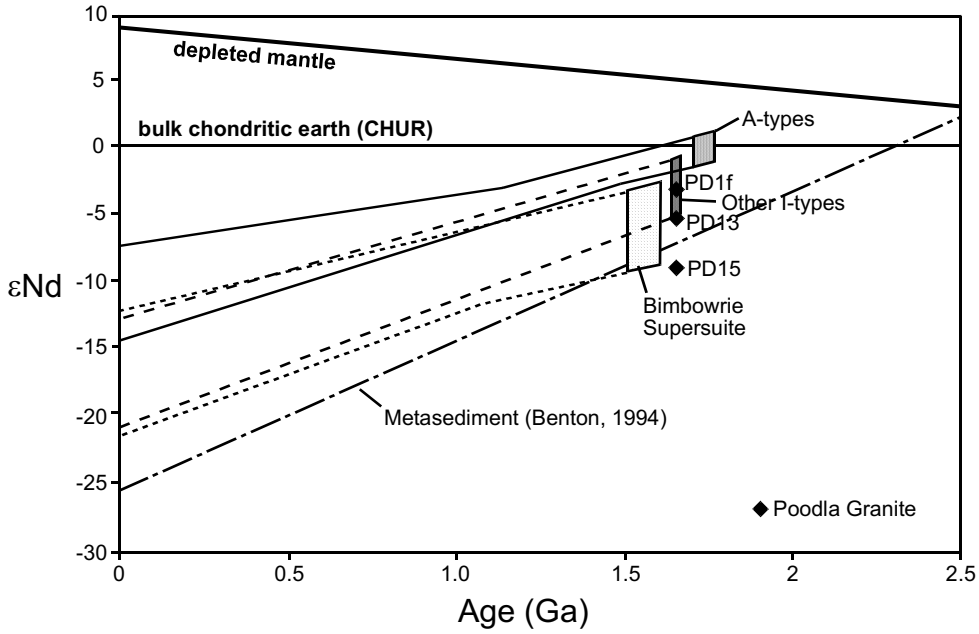
depleted mantle
bulk chondritic earth (CHUR)
A-types
PD1f
Other I-types
PD13
PD15
Bimbowrie
Supersuite
Metasediment (Benton, 1994)
Poodla Granite
εNd
Age (Ga)
10
5
0
-5
-10
-15
-20
-25
-30
0
0.5
1.0
1.5
2
2.5

Figure 14a

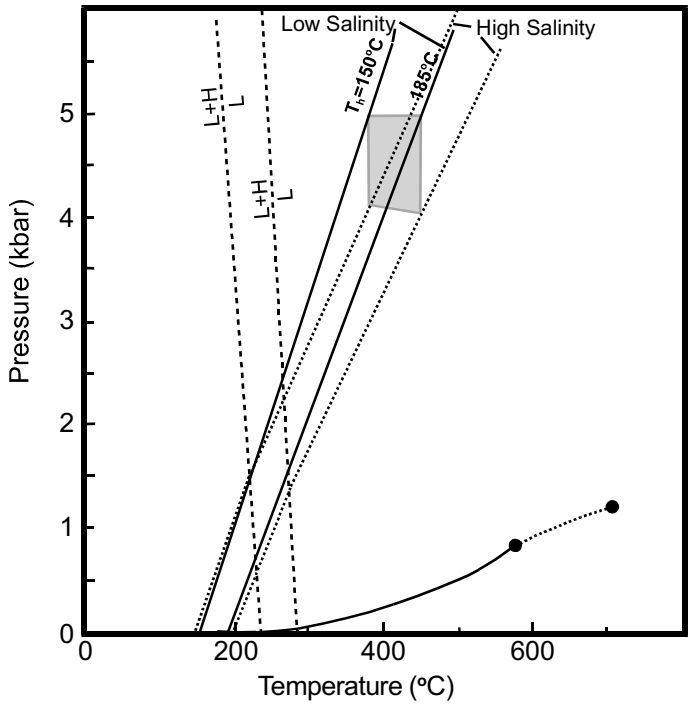
Low Salinity
High Salinity
T_h=150°C
185°C
L+H
L
L+H
L
Pressure (kbar)
0
1
2
3
4
5
0
200
400
600
Temperature (°C)

Figure 14b

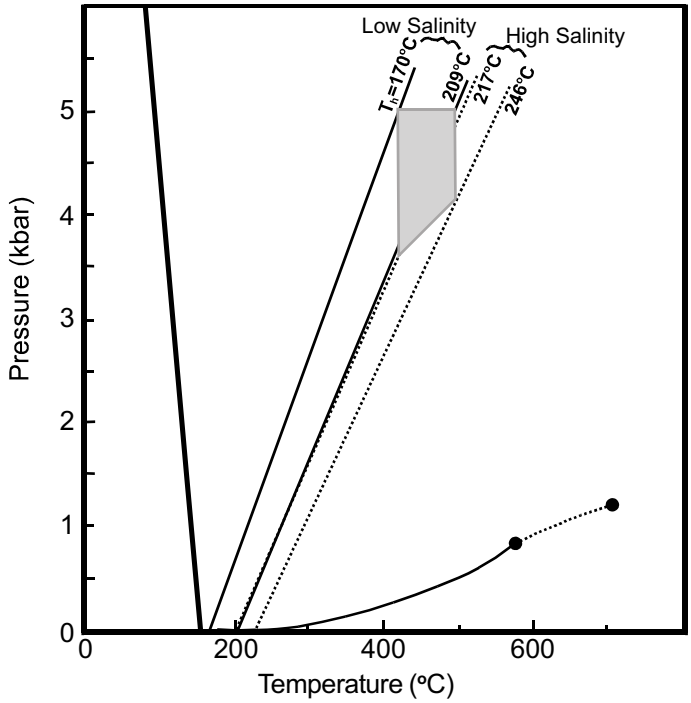
Low Salinity
High Salinity
T_h=170°C
209°C
217°C
246°C
Pressure (kbar)
Temperature (°C)
0
1
2
3
4
5
0
200
400
600

Figure 15

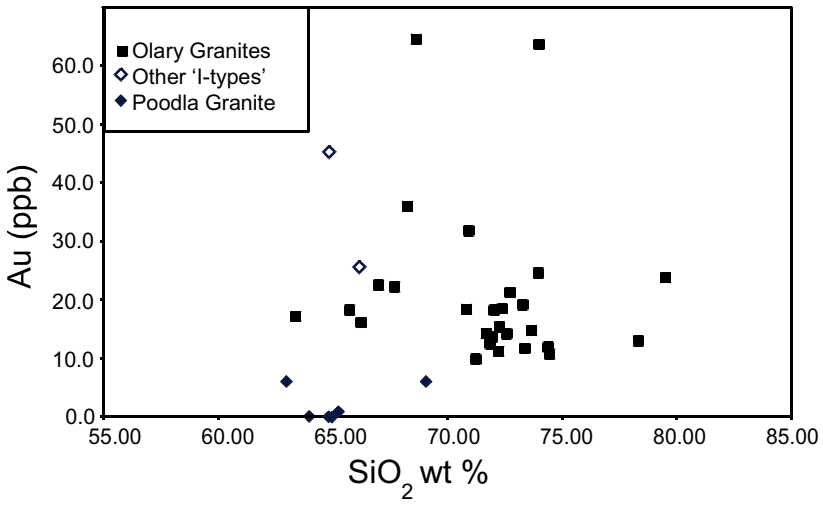
Olary Granites
Other 'I-types'
Poodla Granite
Au (ppb)
60.0
50.0
40.0
30.0
20.0
10.0
0.0
55.00
60.00
65.00
70.00
75.00
80.00
85.00
SiO2 wt %